# A study of data sampling in PET with planar detectors

Thomas Rodet, Johan Nuyts, Michel Defrise, Christian Michel [1]

## I. Introduction

The definition of data sampling in 3D positron emission tomography with multi-crystal scanners occurs at two different levels:

1. The *native sampling* is determined by the set of measured line of responses (LORs) linking the centers of pairs of detectors.
2. The *software sampling* is the set of LORs in which the individual coincidences are histogrammed before being processed for image reconstruction.

Selecting a software sampling which differs from the native sampling entails some loss of resolution due to data interpolation, but allows to generate a regular sampling which is more easily amenable to efficient analytic or iterative reconstruction in a clinically acceptable reconstruction time (cfr in 2D the arc-correction and the reorganization of the native interlaced LORs onto a rectangular sinogram grid). The software sampling also allows to compress low count data by undersampling, both to accelerate computations and to avoid negative values of the true (= prompt - delayed) samples.

The choice of sampling for clinical and animal scanners has been largely empirical, being constrained by the geometry of the crystal blocks and by pre-existing reconstruction software. A more fundamental approach could contribute to a better understanding of the problem, and possibly lead to recommendations for scanner design. Particularly difficult to handle in 3D PET is the data redundancy: using the terminology of multi-ring scanners, the sinograms with ring difference 0 are sufficient, if properly sampled, to exactly reconstruct a band-limited 3D image. At first sight, then, the question of how to sample the redundant, additional data (non-zero ring differences) is poorly defined. Two often overlooked issues then become crucial: the robustness of a given sampling scheme to violation of the band-limited hypothesis, and the stability for noise.

The standard tool in sampling theory is the multi-dimensional generalization of Shannon's theorem [1]. This theorem has been applied [e.g. 2] to parallel-beam and fan-beam sampling in 2D tomography, and to helical CT [3]. In section II, this theorem is applied to 3D PET with planogram sampling. Apart from being a native scheme for scanners with (single layer) panel detectors, the planogram parameterization admits an efficient implementation of voxel driven backprojection [4]. The conditions for sufficient sampling are defined in section II, but we have not yet identified an optimal sampling scheme for this 4D problem with redundant data.

As an initial step, we study in section III the 2D linogram sampling and show that the optimal sampling grid is interlaced. Undersampled schemes are also investigated. In analogy with the linogram-type axial sampling of multi-ring PET scanners, these undersampled schemes correspond to various values of the so-called span factor in the ECAT (CPS) scanners. The odd span factors (implemented in existing scanners) lead to a rectangular linogram grid, whereas the even spans lead to an interlaced grid. We show that the field-of-view (FOV) which can be reconstructed without aliasing is smaller with the odd spans than with even spans.

The main results of this work are: i/ The characterization of the sampling conditions for planogram 3D PET data, ii/ For undersampled 2D linogram sampling, the fact that a larger FOV is allowed by even span than by odd span factors.

[1]T. Rodet and M. Defrise are with Dept. of Nuclear Medicine, Vrije Universiteit Brussel, J. Nuyts is with Dept. of Nuclear Medicine, Katholieke Universiteit Leuven, Belgium. C. Michel is with CPS Innovations, Knoxville, TN.

## II. Data sampling for planograms

We parameterize the 3D x-ray transform using two plane detectors in the planes $y = \pm 1$:

$$g(u, v, u', v') = \int_{-1}^{1} dy\ f(u - yv, y, u' - yv') \qquad (1)$$

which is a weighted line integral linking two points $(x = u \pm v, y = \mp 1, z = u' \pm v')$. The function $f(x, y, z)$ vanishes for $|y| > r$, where $r < 1$ defines the size of the FOV. Our analysis is done for hypothetical stationary and infinite panel detectors, i.e. for $(u, v) \in \mathbb{R}$, and we make the working hypothesis that optimal sampling properties will remain approximately valid for finite panel detectors rotated in a few positions. The 4D Fourier transform of the data is [4]:

$$G_{1111}(U, V, U', V') = \delta(VU' - V'U)\, F_{101}(U, y = -V/U, U') \qquad (2)$$

where upper case characters represent Fourier transforms or conjugate frequencies, and the indices indicate with respect to which variables the transform is taken. If the image is band-limited with maximum frequency $W$, then $G_{1111} = 0$ outside the region

$$K = \{(U, V, U', V') \mid \quad VU' = V'U \quad \text{and} \quad U^2 + U'^2 \leq W^2 \quad \text{and} \quad |V| \leq r|U|\} \qquad (3)$$

Because of data redundancy, $K$ is a 3D manifold in the 4D frequency space. The projection of $K$ onto the $V' = 0$ hyperplane has a shape similar to that studied by Desbat [3] for

helical CT. The Petersen-Middleton theorem can now be stated: if the planogram is sampled on a 4D grid defined by some 4x4 non-singular matrix $\mathcal{S}$, i.e. for the points $(u, v, u', v') = (i, j, k, l)\mathcal{S}^t$, $(i, j, k, l) \in Z^4$, then $g$, and hence $f$, can be recovered exactly provided the copies of $K$ translated by $(\Delta U, \Delta V, \Delta U', \Delta V') = (m, n, p, q)\mathcal{S}^{-1}$, $(m, n, p, q) \in Z^4$ do not overlap. Checking whether two copies overlap in $\mathbb{R}^4$ is complex, but we show that there is overlap if and only if there exist a pair $U, U'$ such that

- $U^2 + U'^2 \leq W^2$, $(U - \Delta U)^2 + (U' - \Delta U')^2 \leq W^2$,
- $r|U\Delta U' - U'\Delta U| > |U\Delta V' - U'\Delta V|$,
- $r|U\Delta U' - U'\Delta U| > |(U - \Delta U)\Delta V' - (U' - \Delta U')\Delta V|$.

Using this simplification, specific sampling schemes can be proposed. The simplest one has a single $v' = 0$ sample, and reduces to a 2D slice-by-slice sampling using data with ring difference 0. Alternative, fully 4D, schemes satisfying the sampling condition will be presented.

## III. Data sampling for linograms

We have analysed the sampling of 2D linograms corresponding to a pair of parallel linear detector arrays. The problem is easily analyzed by restricting to their first two arguments the functions $g$, $G$, $f$, and $F$ in equations (1) and (2). The 2D domain $K = \{(U, V) || U | \leq W$ and $|V| \leq r|U|\}$ is then a truncated cone, with an aperture related to the diameter $2r$ of the FOV. If the individual "crystals" in each array are spaced by a distance $d$, the native $(u, v)$ sampling is interlaced. This scheme satisfies the sampling condition for $W \leq 1/2d$ and $r < 1$, and corresponds to the closest possible packing of copies of $K$. Undersampled schemes average sets of adjacent $v$ native samples. Two approaches are possible (figure 1). The first one generates a rectangular $(u, v)$ grid by averaging sets of $(S - 1)/2$ or $(S + 1)/2$ $v$ samples, for some odd "span" factor $S$. The second generates an interlaced $(u, v)$ grid by averaging sets of $S/2$ $v$ samples for some even "span" factor $S$. In both cases the data storage and the reconstruction time are roughly divided by a factor $S/2$. This data averaging acts as a low-pass filter on the data $g$, but this filter is not an ideal low-pass filter and therefore the support of the Fourier transform $G_{11}$ is still given by the same 2D cone $K$.

We show that the FOV that can be recovered without aliasing is $r = 2/S$ for even span, but only $r = 1/S$ for odd span. Figure 2 shows a simple phantom reconstructed by filtered- backprojection from linogram data undersampled with span 6 and span 7. The aliasing artefacts close to the edge of the image (which covers a FOV of 1/3) are stronger with the odd span, but the resolution is almost identical in the two images. This might be due to the difficulty of accurately implementing FBP with interlaced samples (see [5] for the fan-beam case), but we also show theoretically that the interlaced sampling is more sensitive to violation of the assumption that $f$ is $W-$band-limited. We are further investigating the implications of these results for 3D PET, and are pursuing the full 4D analysis presented in the previous section.

## References


[1] D Petersen and D Middleton, Inf Control 5, 279-323 (1962).
[2] F Natterer, The Mathematics of Computerized Tomography, Wiley 1986.
[3] L Desbat, Proc. 1995 Int. Symp. Fully 3D Reconstruction, Kluwer 1996, 87-102.
[4] D Brasse et al, 2000 IEEE MIC Symposium (paper 15-239).
[5] F Natterer, Numerical Methods in tomography, Acta Numerica vol. 8, S 107-143 (1999).


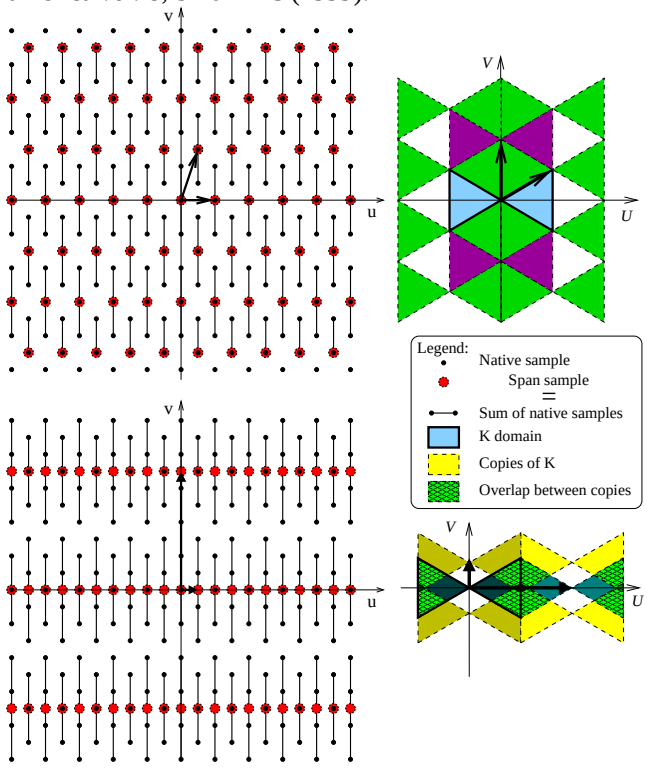


Fig. 1 (Left column) Sampling scheme in the Linogram space (Right column) Packing of $K$ support in the Fourier space for $r = \frac{1}{3}$ (Top) Span 6 Scheme, (Bottom) Span 7 scheme.

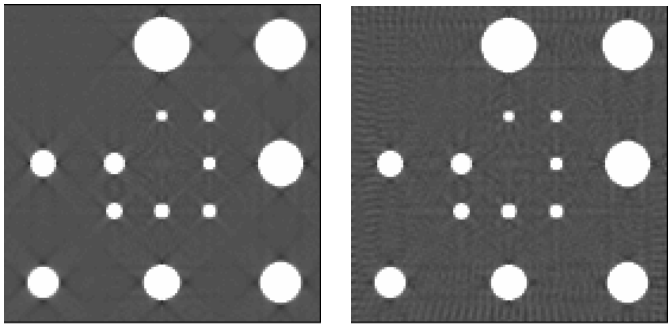

Fig. 2 FBP linogram reconstruction of a 133 × 133 pixels (Left) reconstruction with Span 6: 401 samples along the $u$ axis and 298 along the $v$ axis, (Right) reconstruction with Span 7: 802 samples along $u$ and 126 along $v$. The ramp filter is apodized by a hamming window. The grey scale is at $[-5\%, +10\%]$ of the maximum.